This research was initiated while the first author was on sabbatical leave at the National Water Research Institute. The support provided during this period by Environment Canada, under contract no. OSE18-00253, and by the Gledden Foundation of the University of Western Australia in the form of a Gledden Overseas Fellowship, is acknowledged. Subsequent support was provided by the Centre for Environmental Fluid Dynamics at the University of Western Australia.

THERMAL SIMULATION OF LAKES WITH WINTER ICE COVER

by

J.C. Patterson[1] and P.F. Hamblin[2]

[1]Dept. of Civil Engineering
The University of Western Australia
Nedlands, WA. 6009
Australia

[2]Aquatic Physics & Systems Division
National Water Research Institute
Canada Centre for Inland Waters
Burlington, Ontario

July 1984

NWRI Contribution #85-29

Abstract

A one-dimensional thermodynamic model of a two component ice/snow cover is added to an existing one-dimensional lake mixing model. Emphasis is placed on the thermodynamic coupling between the ice and mixing models which has been absent in previous models. The two-dimensional effects of partial ice cover are incorporated into this one-dimensional framework by using a minimum ice thickness. The model is applied to Lake Laberge, Yukon Territory and to Babine Lake, British Columbia for a period covering the formation and demise of full ice cover. The results of the model are directly compared to snow and ice measurements and indirectly tested by comparison with water column data during the spring period, with good results. This implies that the ice and snow model is performing satisfactorily, and emphasizes the importance of the coupling between the ice and the underlying water. The successful simulation of the observed mixed layer under the ice driven by convective stirring caused by short wave heating below the temperature of maximum-density is an example of the model's ability to provide physical insight into processes occurring in lakes.

Résumé

On a combiné un modèle thermodynamique à variable unique d'une couverture à deux éléments (glace et neige) à un modèle, à variable unique également, du brassage d'eau dans les lacs. La principale caractéristique de cette expérience, qui la distingue des autres qui ont précédé, se trouve dans la combinaison thermodynamique du modèle de couverture glacielle et de celui du brassage d'eau. L'effet bi-dimensionnel de la couverture glacielle partielle a été incorporé à ce modèle à une variable en utilisant une couche de glace d'une épaisseur minimale. Le modèle a été appliqué au lac Laberge, au Yukon, et au lac Babine, en Colombie-Britannique, pendant la période correspondant à la formation et à la disparition complète de la couverture glacielle. Les données obtenues par le modèle ont été comparées à des mesures directes d'épaisseur de la glace et de la neige, ainsi qu'aux données obtenues sur la tranche d'eau au cours du printemps; les résultats se sont avérés satisfaisants. On peut en conclure que le modèle de couverture glacielle et nivale est adéquat et que la combinaison des paramètres glace et eau sous-jacente est un facteur important. Le réchauffement par le soleil de la couche sous la glace à une température inférieure à la densité maximale de l'eau occasionne un mouvement de convection; la simulation réussie de ce brassage est un indice de la capacité du modèle à ajouter à nos connaissances dans les processus physiques qui surviennent dans les lacs.

Introduction

The capability of simulating the vertical distributions of temperature and other water quality parameters in lakes and reservoirs has long been recognized as an important tool for resource management, and many models intended to fulfill this role have been generated with varying degrees of success (Orlob 1984; Harleman 1983). Increasing development of northern regions has, however, added an additional dimension to the simulation problem in that the formation and ablation of a winter ice cover and its interaction with the underlying water must be incorporated.

Although a number of 'freezing day' models of lake ice formation have been described in the literature (e.g. Pivovarov 1973), these are essentially bulk thermodynamic, long time scale models with little or no connection with the lake processes, such as mixing occurring beneath the ice. The definitive thermodynamic model of surface ice formation and ablation appears to be that of Maykut and Untersteiner (1971), who formulated a one-dimensional (1-D) model of the unsteady heat transfer through a two component (ice/snow) cover. The model was directed at modelling sea ice, but was not linked to an oceanic mixing model.

This lack of interaction with the processes in the underlying water meant that one of the boundary conditions for the heat transfer problem, the heat flux across the ice/water interface, was unknown. The authors used specified values for their model runs; however, they noted that the predicted ice thickness was sensitive to the value used. As the value of the flux is not generally known, its specification is a major deficiency in a predictive model.

Semtner (1976) formulated an alternative version of the same model and showed numerically that the assumption of a quasi-steady solution to the heat transfer equations was of sufficient accuracy provided the ice was thin (less than about 1 m). In this case, the steady equations were solved at each time step, with the time variation being incorporated in the boundary conditions. This implies that the temperature distribution has reached steady state before a time step has elapsed. More generally, for thin ice, the time scale for heat conduction through ice of thickness h_i is of order h_i^2/κ_i, where κ_i is the thermal diffusivity, is short when compared with the time scale of changes in the meteorological forcing. The assumption may be formalized for all thicknesses in terms of the Stefan number

$$S = \frac{C\Delta T}{L} \qquad (1)$$

where C is the specific heat, L the latent heat of fusion, and ΔT the characteristic temperature difference. For $S < 1$, the quasi-steady assumption may be shown to be valid (Gilpin et al. 1980: Hill and Kucera 1983).

A number of other specialized forms of essentially the Maykut and Untersteiner (1971) model have been documented. For example Wake and Rumer (1978), Rumer et al. (1981), Hibbler (1979), and de Broissia et al. (1981)

have developed models directed at various aspects of surface ice formation and behaviour, including ice dynamics. None of these models, however, treat the thermodynamic coupling between the ice cover and the underlying water in more than a rudimentary way.

A second unsatisfactory aspect of the Maykut and Untersteiner (1971) model, with respect to lake applications, is its assumption of one-dimensionality. While clearly this assumption greatly simplifies the problem and may be appropriate for sea ice applications, it is not a good assumption during freezing and melting periods in lakes when large areas of open water typically exist. These open areas have different surface heat flux characteristics to the ice covered areas and therefore influence the thermodynamic processes in the water; consequently, the thermodynamic coupling between ice and water is modified, affecting the rate of freezing or melting.

In this paper, a two component (ice/snow) model based on the Maykut and Untersteiner (1971) formulation is linked to a reservoir mixing model, thus capturing the thermodynamic coupling. The coupling is in both directions; the mixing model determines the heat flux at the interface, affecting the ice characteristics. In turn, the characteristics of the ice cover provide boundary conditions for the mixing model. Further, by assuming a minimum thickness at which ice can exist on the surface, the properties of a partial ice cover are incorporated. Thus ice formed over the full surface at a thickness less than the minimum is assumed to be transported, by for example the surface wind stress, to accumulate at the minimum thickness. The open and covered areas have different surface heat transfer characteristics and the underlying water will respond differently. The adjustments to the horizontal gradients in density established in this way are assumed to occur rapidly, and the mixing model becomes 1-D, while retaining the effects of the different heating rates appropriate to ice and open water.

Little data with reference to the ice cover on lakes appears to have been documented. Although some data on small northern and arctic lakes exists (e.g. Schindler et al 1974), the only complete data set for a medium sized lake known to the authors is that for Babine Lake, British Columbia (Farmer 1975; Farmer and Carmack 1981; Lee 1977). These data were directed at mixing processes beneath the ice and only scattered information on the ice/snow conditions is available. This precludes a direct comparison between model and measured values of ice conditions; however, the intensity and quality of the water column data means that indirect and, in view of the complex interaction between the ice cover and the water, perhaps more stringent comparisons may be made.

Thus we refer to a set of more recent observations of snow and ice thickness made in a medium size lake, Lake Laberge Yukon Territory, for a more detailed comparison of the modelled ice conditions.

The Babine Lake data were made available in edited form by Dr. D. Farmer of the Institute of Ocean Sciences, Patricia Bay, B.C. The authors acknowledge his assistance in providing and interpreting these data.

The two component ice/snow model

Ice/snow thermodynamics - Following Maykut and Untersteiner (1971), the distribution of temperature through the two-component cover is described by

$$K_i \frac{\partial^2 T_i}{\partial z^2} + \lambda_i I_o e^{-\lambda_s h_s - \lambda_i (h_i - z)} = 0 \qquad 0 \leq z \leq h_i$$

$$K_s \frac{\partial^2 T_s}{\partial z^2} + \lambda_s I_o e^{-\lambda_s (h_i + h_s - z)} = 0 \qquad h_i \leq z \leq h_i + h_s \tag{2}$$

where the subscripts i and s refer to ice and snow respectively. In Eq. 2 T is the temperature as a function of z, the distance above the ice-water interface (Fig. 1), K the thermal conductivity, λ the extinction coefficient for short wave radiation, and h the component thickness. I_o is the non-reflected short wave radiation intensity at the upper surface; for an incident radiation intensity Q_o, $I_o = (1 - a)\ Q_o$, where α is the surface albedo. The albedo of short wave radiation is well known to be a strong function of snow age and snow temperature. This dependence is modelled herein after the empirical curves given by the U.S. Corps of Engineers (1956).

The boundary conditions on Eq. 2 may be written as

$$
\begin{aligned}
T_i &= T_f && z = 0 \\
T_i &= T_s && \\
K_i \frac{\partial T_i}{\partial z} &= K_s \frac{\partial T_s}{\partial z} && z = h_i \\
T_s &= T_o && z = h_i + h_s
\end{aligned}
\qquad (3)
$$

where T_f is the freezing temperature of the surface water and T_o the upper surface temperature, yet to be determined.

Equations 2 and 3 embody the quasi-steady assumption. In principle, T_o, h_i, and h_s are functions of time, and Eq. 2 should contain an unsteady term. The assumption however implies that the temperature distributions stabilize on a time scale much shorter than that of variations in T_o or the thicknesses. This allows a decoupling of the thermodynamic balances at the surface and the ice/water interface. Since these balances both depend on heat fluxes, an explicit expression of the solution of Eqs. 2 and 3 is not necessary.

The surface flux condition - At the atmospheric interface, both meteorological heat fluxes and the heat flux in the upper component are present. Any imbalance in these fluxes must be utilized in heating or cooling of the surface. Thus if there is a net loss of heat at the surface, T_o will decrease until the fluxes balance. On the other hand, an excess of heat will result in a rise in T_o; however, T_o is limited to T_m, the melting temperature of the upper component. Thus some of the excess will be utilized in raising T_o to T_m and the remainder in melting at the surface.

This condition may be expressed as (see Fig. 1)

$$q_o(T_o) + H(To) = 0 \qquad T_o < T_m$$
$$= -\rho L \frac{dh}{dt} \qquad T_o = T_m \tag{4}$$

where q_o is heat flux at the surface of the upper component and H the net meteorological flux, ρ the surface component density, t is time, and h and L refer to the upper component thickness and latent heat of fusion respectively.

A first integral of Eq. 2 yields, for $z = h_i + h_s$,

$$q_o = \frac{K_i K_s (T_f - T_o) + I_o\left(K_i h_s + K_s h_i - \frac{K_i\left(1-e^{-\lambda_s h_s}\right)}{\lambda_s} - \frac{K_s\left(1-e^{-\lambda_i h_i}\right)e^{-\lambda_s h_s}}{\lambda_i}\right.}{K_i h_s + K_s h_i} \tag{5}$$

which, for the case of no snow ($h_s = 0$), collapses onto the appropriate single component (ice) expression. The net atmospheric flux H is given by

$$H = L_I - L_o(T_o) + Q_C(T_o) + Q_E(T_o) \tag{6}$$

where L_I and L_O are the incoming and outgoing long wave radiation intensity, Q_C the conductive heat flux between surface and atmosphere, and Q_E the evaporative heat flux (Fig. 1). The short wave term I_O both enters and leaves the interface, but enters the balance through Eq. 5.

The heat fluxes required by Eq. 6 are given by the usual bulk aerodynamic formulae (TVA 1972) as specified by Imberger and Patterson (1981). The only modification required was the calculation of a vapour pressure over ice or snow, as given by TVA (1972).

The first part of Eq. 4 then results in a non-linear equation for T_o, provided $T_o < T_m$. If this cannot be achieved, $T_o = T_m$ and the second part of Eq. 4 is utilized to melt the surface. Further, Eq. 4 provides only for melting at the surface. It is assumed that there is no mechanism for ice growth at the surface and an increase in snow thickness is taken to occur only through precipitation.

The ice/water interface flux condition - Both ablation and accretion of ice may occur at the ice/water interface. The interface temperature T_f is fixed by the properties of the water; the flux of heat in the ice at the interface depends therefore on T_f and the surface conditions. This flux may be expressed as, from Eq. 2

$$q_f = q_o - I_o\left(1 - e^{-\left(\lambda_s h_s + \lambda_i h_i\right)}\right) \tag{7}$$

depending on T_o and hence the surface conditions through q_o. Independently, the flux of heat from the water to the ice q_w depends only on conditions beneath the ice; an imbalance between these fluxes provides a mechanism for freezing or melting. Thus

$$q_f - q_w = \rho_i L_i \frac{d\, h_i}{dt} .$$

In the Maykut and Untersteiner (1971) model, q_w is specified as a parameter, isolating the ice formation and ablation from the underlying water. In this paper, q_w is assumed to consist of a laminar and turbulent transport

$$q_w = q_\ell + q_s \tag{9}$$

where the laminar flux, q_ℓ, $q_\ell = -K_w \, \partial T_w/\partial z\big|_{z=0}$
where T_w is the water temperature as a function of z, determined by the lake mixing model, and K_w the molecular conductivity. Sensible heat transfer is added to the molecular component following the standard bulk aerodynamic approach.

$$q_s = C_s \rho_w C_p \, U \left(T_w - T_f\right)$$

where ρ_w is the water density, C_p the specific heat of water, U the speed of the flow in the uppermost layer ice and C_s is the sensible heat transfer coefficient or Stanton number. Gilpin et al. (1980) established that C_s varied between 0.6 and 1.0 x 10^{-3} in a laboratory experiment while Hamblin (1985) determined a value of C_s of 1.4(8) x 10^{-3} from field measurements in two ice covered lakes. The depth of which U and T_w were specified was 1 m. The later value is used in the subsequent simulations. In Babine Lake there is no through flow during the period considered, so that only q_ℓ applies while in the riverine Lake Laberge q_s dominates. The water temperature must increase from T_f to T_w over some thermal boundary layer, and provided T_w is less than the temperature of maximum density, the resulting stratification is stable. The measurements of Farmer (1975) indicate that this boundary layer occurs over length scales of 15-30 cm, and with a characteristic temperature difference of a few degrees, the stratification is sufficiently strong to inhibit turbulent mixing. The assumption of a molecular value of K_w is therefore not unreasonable for Babine Lake.

Model description

A simple, 1-D model of ice/snow formation and ablation is described by Eqs. 2-9 above, with thermodynamic coupling to the lake processes through Eq. 9. With such a model, the first ice created will be in the form of an extremely thin sheet covering the entire lake surface. This may occur in sheltered or calm conditions, however, the usual observation is that this ice is transported to the boundaries, and then extends into the lake as cooling continues. Because of the different heat exchanges occurring at water and ice surfaces, it is necessary to parameterize this effect.

To incorporate the effects of this partial ice cover, a minimum ice thickness is specified. As ice forms at a thickness less than this value over the open water, this volume of ice is transported to a smaller area at the minimum thickness, leaving a fraction of the surface as open water. As further freezing occurs, this fraction decreases as the new ice is added to the partial ice cover at the minimum thickness. Thickening of the ice beyond the minimum thickness does not occur until the surface is fully covered.

The minimum thickness is likely to be a function of the mechanism transporting the ice, the surface wind stress or underflow beneath the ice, for example, and is therefore a problem in ice dynamics. This aspect is not pursued in this paper. In the present model, a fixed value of 10 cm has been chosen as being typical for medium sized northern lakes.

The effect of the partial ice cover is to proportionately reduce the wind stirring. In both applications the resultant friction velocity required in the mixed layer formulation was set to zero at complete ice cover. However, in instances of very large winter through flow, as might be the case of a hydroelectric storage reservoir, the friction velocity could be related to the speed of flow of the uppermost layer.

The thickness of the snow overlying the ice cover is limited by the ability of the floating ice to support the snow mass. A simple force balance (Pivovarov 1973) yields for the maximum snow thickness

$$h_{sm} = h_i \frac{(\rho_w - \rho_i)}{\rho_s} \tag{10}$$

where ρ is the density, and the subscripts w, i and s refer to the surface water, ice and snow. Since h_s can only increase by precipitation, any snowfall which would increase h_s beyond h_{sm} is added to the water column as water at temperature T_f, as is precipitation of snow over open water.

The ice/snow algorithm resulting from the parameterization above was added to the lake mixing model DYRESM. This model has been extensively described in the literature (Imberger et al. 1978; Spigel and Imberger 1980; Imberger and Patterson 1981; Ivey and Patterson 1984; Patterson et al. 1984) and only a brief description is warranted here.

The model is based on a Lagrangian layer scheme in which the lake is represented by a series of horizontal layers each of uniform property but variable thickness. The layer positions may change as inflow or outflow modify the lake volume, and individual layer thicknesses are determined by the algorithm to give a resolution appropriate to the process acting on the layers at each time step. The time step itself is variable between 15 minutes and 12 hours, the actual value depending on the time scale of the process operating. Thus the model is able to resolve time scales down to 15 minutes and length scales down to a few centimetres; however, it achieves these resolutions only when and where necessary, resulting in an accurate yet economical model.

For the Babine Lake application, only the mixed layer dynamics and deep turbulent mixing algorithms are relevant at the inflows and outflows in the period considered are negligible. On the other hand, the strong winter flow of the Yukon River through Lake Laberge (140 m^3/s) results in a significant scavenging of heat from the lake. Mixed layer deepening is modelled by the parameterization of the processes of convective overturn resulting from surface cooling (or heating below the temperature of maximum density), wind stirring at the surface, seiche induced shear at the pycnocline, and billowing at the pycnocline resulting from shear instability. Turbulent transport in the hypolimnion is modelled by a diffusion like process, with an eddy diffusivity depending on the local density gradient and the rate of dissipation of turbulent kinetic energy.

The parameterizations of these processes and the architecture of the model have been discussed at length in the references cited. In particular, Imberger and Patterson (1981) give a detailed description of the model structure and its application. This reference also gives values of all of the energy conversion efficiencies, which were not changed for this application.

To this basic 1-D model structure was added the ice/snow model described above. The 1-D nature of the model is retained by keeping the partial ice as a fraction of surface area covered; the surface heat transfers are performed separately in open water and ice covered areas, and any horizontal density gradients immediately relaxed. Since partial ice implies an ice thickness of 10 cm, the upper layer in the open water is maintained at this thickness, with horizontal adjustments occurring below this level.

Heat flux from the underlying sediments to the bottom water has been identified as an important component of the winter thermodynamics of small lakes (Mortimer and Mackereth (1958); Welch and Bergmann (1985). Since both lakes of present interest are deep medium sized lakes, we have set the bottom heat flux to zero in the model.

The model requires as inputs daily values of average wind speed, air temperature and humidity, daily inputs of incoming long and short wave radiation intensity, and rain and snowfall. The model is initialized by a specified temperature profile obtained from the field data and allowed to run without interference for the extent of the data. Subsequent field profiles of temperature are used for comparison purposes only.

Lake Laberge simulation

We first describe the results of the Lake Laberge application as snow and ice measurements are available on two occasions during the 1982-83 winter season. A location chart, Fig. 2 also shows that the daily meteorological inputs were from Whitehorse about 50 km south of the lake proper. Incoming longwave radiation was estimated from measured total and short wave radiation. Daily inflows and outflows were measured in reasonable proximity to the lake by Water Survey of Canada but unfortunately inflow temperatures were unavailable and had to be estimated by a riverine temperature model. Initial temperatures of the lake were unknown but estimated to be isothermal at 4°C shortly after spring breakup. A light extinction coefficient of 0.35 m^{-1} for the water was assumed. Snow and ice readings were measured at ten locations across the lake on each of two occasions.

Predicted and observed snow and ice thicknesses are presented in Fig. 3. Unfortunately, observations of the dates of first appearance of ice and complete freeze up are not available for Lake Laberge but for the Yukon River at Whitehorse ice was first observed on 7 November covering the river by 23 November. The simulated date of first appearance of lake ice was 10 November while complete ice cover was reached by 26 November. In consideration of the larger thermal capacity of the lake compared to the river, this agreement is encouraging. Parenthetically it may be noted that an assumed input of river borne frazil ice formed during the period of river freeze up had very little effect on the rate of freezing over of Lake Laberge and at most would advance the above dates by one day. However, this affect may be important in smaller lakes or cases where the inflowing river remains open at 0° for most of the winter period.

Modelled snow and ice thickness are within the observational error on both occasions lending confidence to the ability of the above described algorithm to treat the thermodynamics of ice covered lakes. Having established the accuracy of the method for treating ice cover, we turn to a second example where water temperature observations are available under the ice.

Babine Lake simulation

The field program and resulting data from the Babine Lake study are fully described by Farmer and Spearing (1975), Lee (1977), Farmer (1975), and Farmer and Carmack (1981), and will not be further discussed here. As noted above, these data were obtained with a view to a study of the mixing processes beneath the ice, and virtually no information on the characteristics of the ice and snow cover is available. A map of the lake is shown in Fig. 4; although thermistor chains were deployed at a number of stations for various periods, the only continuous record through winter was available from the station shown. Data from this site was used to initialize the model and for subsequent comparisons with model predictions.

The simulation was run from 26 December 1973 to 31 May 1974, a total of 156 days, spanning the formation and disappearance of ice cover. This period was chosen for analysis rather than the previous winter period studied by Farmer (1975) on account of the availability of concurrent meteorological records. Although data are available prior to this period, only modelling of the ice physics was of interest. The meteorological station failed with the onset of significant ice cover on 31 December; subsequent data were obtained from nearby meteorological stations at Pinkut Creek and Smithers Airport. The variation of some of the meteorological forcing (average daily wind speeds and air temperature and total daily solar radiation) over the simulation period are shown in Fig. 5. Longwave radiation was estimated from the standard formula, Imberger and Patterson (1981). The light extinction coefficient was taken from Farmer and Spearing (1975) to be 1.0 m^{-1}.

The data from the thermistor chain are shown as isotherm depth histories in Fig. 6a. The uppermost thermistor of the chain also failed on 31 December and the interpolation procedure used to generate the figure is unable to represent events above the level of the second thermistor, at a depth of 7 m beyond that date. The broken line in Fig. 6a is at this 7 m level. The actual date of full ice cover is not known, however, the failure of the meteorological station and the upper thermistor on 31 December indicate the presence of significant ice in the centre of the lake. Consequently, 1 January is taken as the date of full ice cover. This estimate is supported by the rapid drop in air temperatures (Fig. 5) and cooling in the upper 40 m (Fig. 6a) preceding this date.

Following the formation of full ice cover, there is very little activity in the water column (Carmack and Farmer 1982) which is now protected from surface event by the ice cover until the following spring. In view of the extremely weak temperature gradient, the small fluctuations evident in the isotherm depths correspond to very small local temperature fluctuations. In mid April the increasing short wave radiation is able to penetrate the ice cover and warm the water below; as this water is below 4°C, the result is unstable and a mixed layer forms, evidenced by the upturn in the 1.5°C isotherm. As the mixed layer deepens, the 2.0, 2.5, and 3.0°C isotherms surface. The thermistor chain data does not continue sufficiently long to show the upturn of the 3.5°C isotherm. As this mixed layer deepening is the result of short wave radiation penetrating the ice, it is extremely sensitive to the thickness of the ice and snow cover as well as their transmission properties.

The results of the simulation are presented in the same format in Fig. 6b. The model was initialized with the thermistor chain data on 26 December and run for 156 days, the extent of the meteorological data. The rapid cooling prior to 31 December does not extend to the depth indicated in Fig. 6a, however, full ice cover is predicted on 31 December. The predicted isotherm depths remain horizontal for much of the period, but without the small fluctuations evident in Fig. 6a. As noted above, these fluctuations represent extremely small temperature fluctuations. As the water column is protected by the surface ice, this prediction of constant isotherm depths is not surprising nor a good test of the model. The timing of the surfacing of the 1.5, 2.0, 2.5, and 3.0°C isotherms is however almost exactly that indicated by the data, resulting from warming and mixing beneath the ice.

This radiation penetration and resultant mixing depends strongly on the snow and ice thicknesses and the reflection and absorbtion properties. The model uses published values of the latter parameters; the achievement of the desired result means that, at the onset of mixing, the model has predicted the correct values of ice and snow thickness. That the subsequent deepening of the mixed layer is also well predicted means that the rate of melting of both ice and snow is accurately modelled. This close correspondence near the end of the simulation and the prediction of full ice on 31 December in addition to the Laberge simulation strongly suggests that the ice/snow algorithm accurately models the formation and ablation of ice and snow over the full period.

The performance of the model during this period of radiation induced mixing beneath the ice is shown in more detail by the series of field and predicted profiles in Fig. 7. A comparison of the profiles shows that the model accurately predicts the field values on a daily basis, both in terms of the deepening of the mixed layer and the absolute values of temperature.

This mechanism may be viewed in another way. Figure 8 shows the difference between the short wave radiation actually reaching the underside of the ice, q_{sw}, and the heat flux from the water to the ice, q_w. The first term causes heating of the water and the second cooling; if the difference is positive, mixing occurs. Figure 8 clearly shows the rapid onset of this mechanism during April, indicating a critical combination of cover thickness and radiation intensity. Once begun, the mechanism is self perpetuating as long as the intensity of the radiation reaching the water increases. Mixing below the ice brings relatively warm water to the interface, increases q_w and causes melting at the interface. The reduced thickness then allows more radiation to pass through the ice and the process continues.

During the period of mixed layer growth when $q_{sw}-q_w$ is positive, we may estimate the effective convective velocity scale, w* (Imberger and Patterson 1981) from the mixed layer depth and the heating rate. This scale ranges from 0.2 cm/s on April 17 to 0.4(3) cm/s at the end of April 1974 and is in close agreement with the velocity scale estimated by Farmer (1975) for the previous winter period. This scale velocity may be compared to the overall mixed layer deepening rate of 2.17×10^{-3} cm/s which is considerably less than w* due to requirement for the convective stirring to increase both the potential energy and the turbulent kinetic energy of the mixed layer in the deepening process.

The predicted ice and snow thicknesses are shown in Fig. 9 for the period of ice cover. Although in the case of Babine Lake these results are not comparable to field data, they are typical of the behaviour expected. In particular, the insulating nature of the snow layer is clearly evident, with the rate of change of ice thickness depending strongly on the inverse of the snow thickness. It also may be noted from inspection of Figs. 5 and 9 that the snow disappears rapidly once the mean daily air temperature reaches the melting point.

Discussion

A thermodynamic model of the formation and ablation of an ice and snow cover has been added to an existing 1-D mixing model applicable to lakes and reservoirs. By using a minimum ice thickness, the two-dimensional effects of partial ice cover have been incorporated in this 1-D framework. A direct comparison of predicted ice and snow thicknesses was possible in one case, while in the other, performance of the model has been validated indirectly by testing the influence of the ice cover on the underlying water, for which high quality data exists. This procedure is a stringent test of the ice and snow model, the parameterization of the coupling between the ice and the water, and the mixing model. On all counts the model has performed satisfactorily.

The importance of the interaction between the ice cover and the water column is obvious. The rate of formation of ice depends in part on the heat flux between water and ice, however, the most dramatic effect is under-ice mixing induced in spring. This mixing, bringing relatively warm water to the ice-water interface, is the dominant mechanism for melting of the ice cover and prediction of the disappearance of the ice then depends critically on the parameterization of this process. Models which use externally specified heat fluxes from water to ice cannot realistically model this process.

Although the main objective in the model development was the problem of water quality simulation in lakes and reservoirs, the process orientated approach followed in its construction has allowed an interpretation of an interesting physical process in an ice covered lake to be advanced. Not only are the physics of the mixed layer advance discussed in Farmer's (1975) study of free convection in Babine Lake embodied in our model but also for the first time quantitative estimates of the driving force for this phenomenon, that is the short wave radiation reaching the top of the water column, are possible as well as the ability to relate this driving force to the background environmental conditions. The establishment of the quantitative connection between the general environmental conditions and such a process as the under ice mixing ought to permit reliable application of the model to other water bodies.

References

de Broissia, M., J.M. Baldasano, and B. Coupal. 1981. Modelling the formation and melting of ice cover for the Desaulaiers Reservoir. Simulation Proc. Series., Soc. for Computer Simulation, **9** :39-44.

Carmack, E.C. and D.M. Farmer. 1982. Cooling processes in deep, temperate lakes: A review with examples from two lakes in British Columbia. J. Marine Res., Vol. 40 Supplement p. 85-111.

Farmer, D.M. 1975. Penetrative convection in the absence of mean shear. Quart. J. Roy. Meteor. Soc. **101** :869-891.

_____________, and E. Carmack. 1981. Wind mixing and restratification in a lake near the temperature of maximum density. J. Phys. Oceanogr. **11** :1516-1533.

_____________, and T. Spearing. 1975. Isotherm plots of Babine Lake during the ice free season. Institute of Ocean Sciences, Patricia Bay, B.C. Unpublished report.

Gilpin, R.R., T. Hirata, and K.C. Cheng. 1980. Wave formation and heat transfer at an ice-water interface in the presence of a turbulent flow. J. Fluid Mech. **99** :619-640.

Hamblin, P.F. 1985. Yukon River headwater lakes study, 1983-1985: Preliminary analysis and data report. Unpublished Report, National Water Research Institute, Burlington, Canada.

Harleman, D.R.F. 1981. Hydrothermal analysis of lakes and reservoirs. J. Hydraul. Div. Am. Soc. Civ. Eng. **105** :533-545.

Hibbler, W.D. 1979. A dynamic thermodynamic sea ice model. J. Phys. Oceanogr. **9** :815-846.

Hill, J.M., and A. Kucera. 1983. Freezing a saturated liquid inside a sphere. Int. J. Heat Mass Transfer, **26** :1631-1638.

Imberger, J., and J. Patterson. 1981. A dynamic reservoir simulation model: DYRESM5, p. 310-361. In H.B. Fischer (ed.), Transport models for inland and coastal waters. Academic.

______________, J. Patterson, B. Hebbert, and I. Loh. 1978. Dynamics of reservoir of medium size. J. Hydraul. Div. Am. Soc. Civ. Eng. **104** :725-743.

Ivey, G.N., and J.C. Patterson. 1984. A model of the vertical mixing in Lake Erie in summer. Limn. and Oceanogr. **29** :553-563.

Lee, A.Y.P. 1977. Physical limmology of Babine Lake: data summary 1972-1974 Parts 1 and 2. Institute of Ocean Sciences, Patricia Bay, B.C. Unpublished report.

Maykut, G.N., and N. Untersteiner. 1971. Some results from a time dependent, thermodynamic model of sea ice. J. Geophys. Res. **83** :1550-1575.

Mortimer, C.H., and F.J.H. Mackereth. 1958. Convection and its consequences in ice-covered lakes. Verh. Internat. Ver. Limnol. XIII. pp. 923-932.

Orlob, G.T. 1983. Mathematical modelling of water quality: streams, lakes and reservoirs. Wiley.

Patterson, J.C., P.F. Hamblin, and J. Imberger. 1984. Classification and dynamic simulation of the vertical density structure of lakes. Limn. and Oceanogr. Vol. 29(4), pp 845-861.

Pivovarov, A.A. 1973. Thermal conditions in freezing lakes and reservoirs. Wiley.

Rumer, R.R., A. Wake, S-H. Chieh, and R.D. Crissman. 1981. Development of an ice transport model for Great Lakes application. Proc. 6th Intl. Conf. on port and ocean engineering under ice conditions. **2** :892-901.

Schindler, D.W., H.E. Welch, J. Kalff, G.J. Brunskill, and N. Kritsch. 1974. Physical and chemical limnology of Char Lake, Cornwallis Island (75°N Lat.). J. Fish. Res. Board Canada, **31** :585-607.

Semtner, A.J. 1976. A model for the thermodynamic growth of sea ice in numerical investigations of climate. J. Phys. Oceanogr. **6** :379-389.

Spigel, R.H., and J. Imberger. 1980. The classification of mixed-layer dynamics in lakes of small to medium size. J. Phys. Oceanogr. **10** :1104-121.

Tennessee Valley Authority. 1972. Heat and mass transfer between a water surface and the atmosphere. Div. of Water Resources Research, T.V.A. Report No. 14.

U.S. Corps of Engineers, North Pacific Division. 1956. Snow Hydrology. Summary report of snow investigations, 433 p.

Wake, A., and R.R. Rumer. 1978. Development of a thermodynamic model for the ice regime of Lake Erie. Proc. IAHR Symp. on Ice Problems, Leula, Sweden.

Welch, H.E. and M.A. Bergmann. 1985. Water circulation in small arctic lakes in winter. Can. J. Fish. Aquat. Sci. Vol. 42, pp. 506-520.

Legends to Figures

Fig. 1 The two component ice/snow model, showing the heat fluxes at each interface.

Fig. 2 Lake Laberge shows the location of the meteorological station, o, and the ice and snow observations, x.

Fig. 3 Observed and simulated ice and snow thicknesses, Lake Laberge, Y.T. Error bars of the field observations are shown.

Fig. 4 Babine Lake, shows the location of the main thermistor chain and meteorological station. Reproduced from Farmer and Carmack (1981), by permission of the authors.

Fig. 5 The meteorological forcing for the period considered; daily total short wave radiation, daily average air temperature, and daily average wind speed.

Fig. 6 Isotherm depth histories: A - From the thermistor chain data, B - From the model predictions.

Fig. 7 Temperature profiles for the period of the spring under-ice mixing 14 April to 4 May 1974: A - From the thermistor chain data, B - From the model predictions. Bottom temperature 3.59°C in all cases, surface temperature as indicated.

Fig. 8 The difference between the short wave radiation beneath the ice and the water to ice heat flux. A positive value indicates warming and mixing.

Fig. 9 The predicted snow and ice thicknesses.

Table 1 Ice and snow parameters

Parameter	Symbol	Value
Ice albedo	α_i	0.25
Snow albedo	α_s	from 0.85 (new, cold, freezing) to 0.4 (old, melting)
Extinction coefficient (ice)	η_i	1.5 m^{-1}
Extinction coefficient (snow)	η_s	6 m^{-1}
Thermal conductivity (ice)	K_i	2.3 W m^{-1} $°C^{-1}$
Thermal conductivity (snow)	K_s	0.31 W m^{-1} $°C^{-1}$
Density (ice)	ρ_i	917 kg m^{-3}
Density (snow)	ρ_s	330 kg m^{-3}
Latent heat	L	334 x 10^6 J kg^{-1}

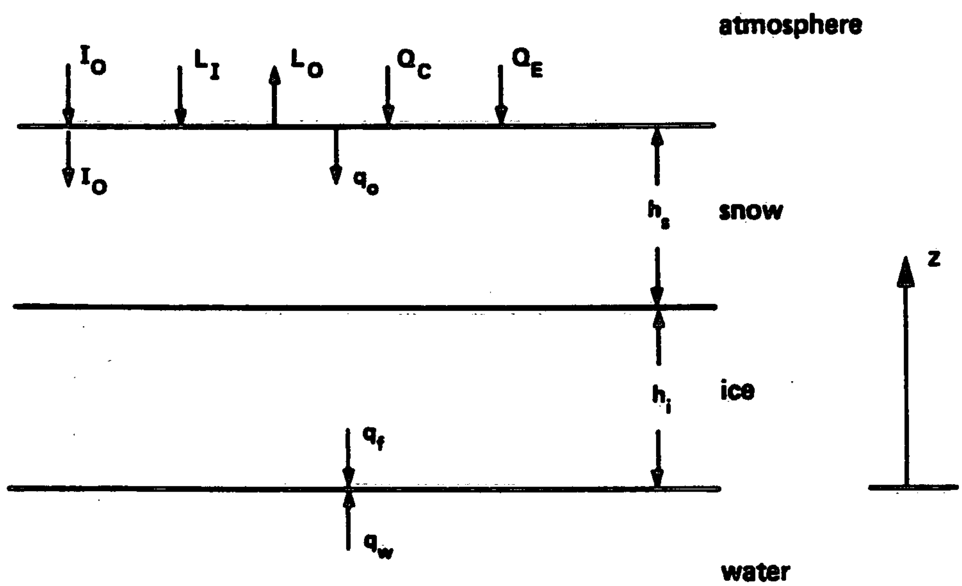

Fig 1

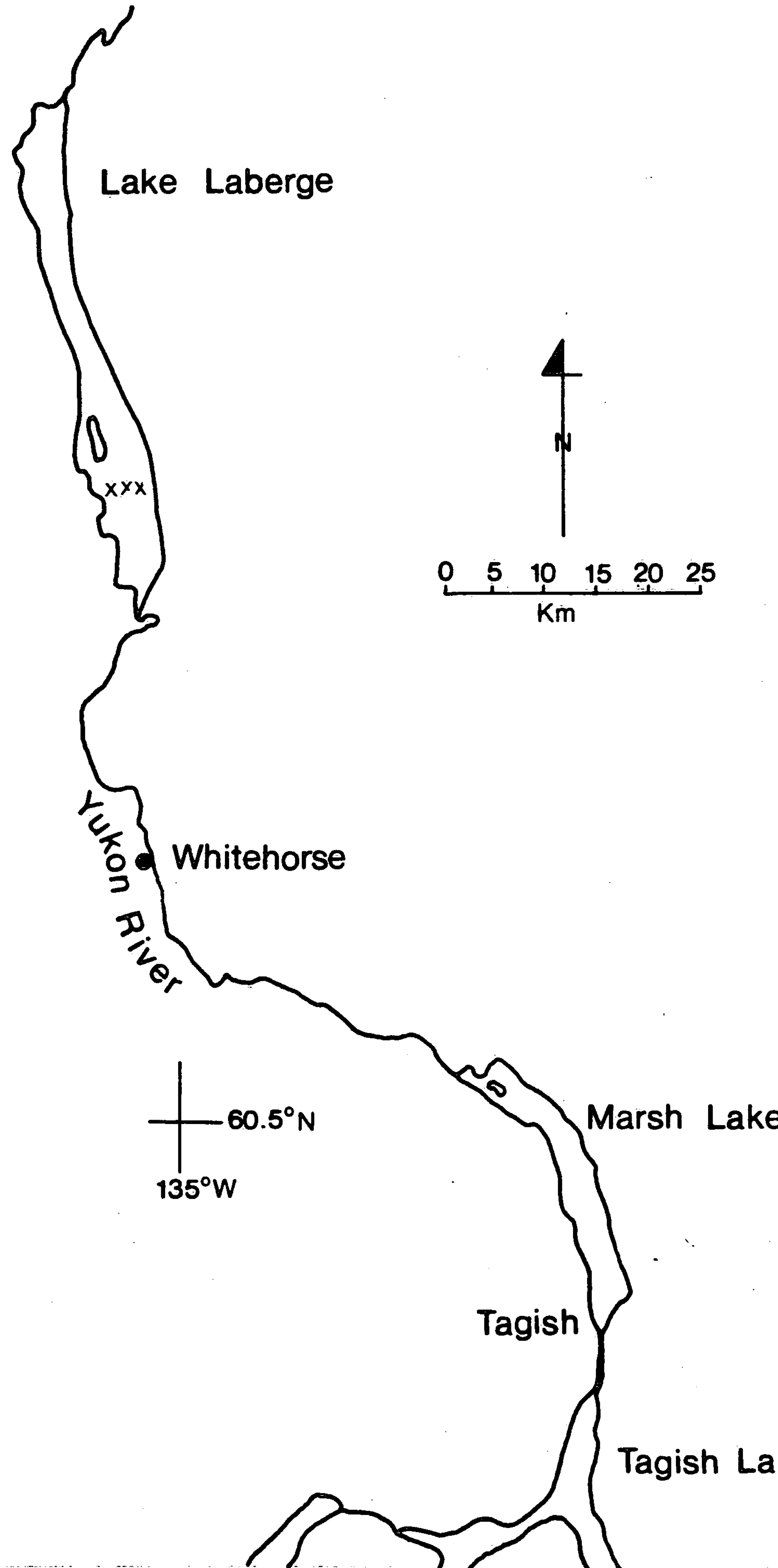
Lake Laberge
XXX
N
0 5 10 15 20 25
Km
Yukon River
Whitehorse
60.5°N
135°W
Marsh Lake
Tagish
Tagish Lake

Fig 2

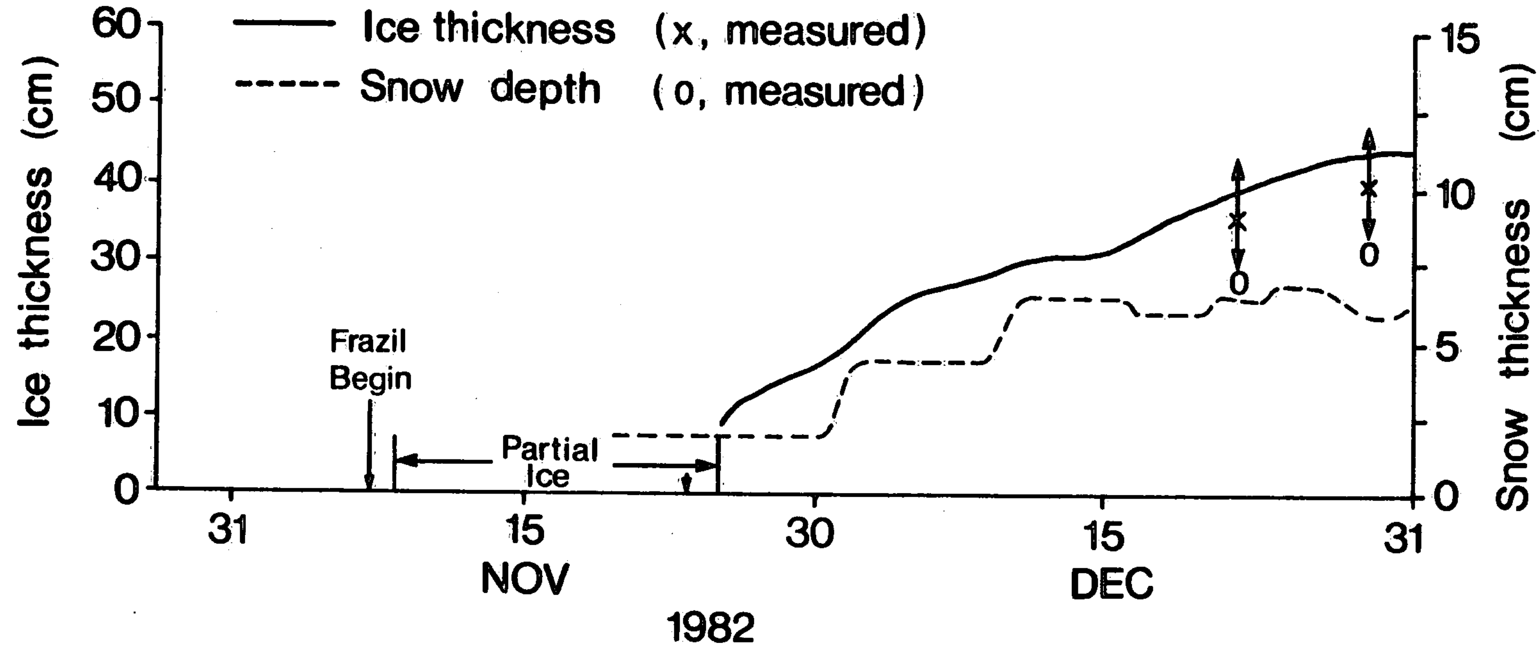
Ice thickness (x, measured)
Snow depth (o, measured)
Ice thickness (cm)
Snow thickness (cm)
60
50
40
30
20
10
0
15
10
5
0
Frazil Begin
Partial Ice
31
15
30
15
31
NOV
DEC
1982

Fig 3

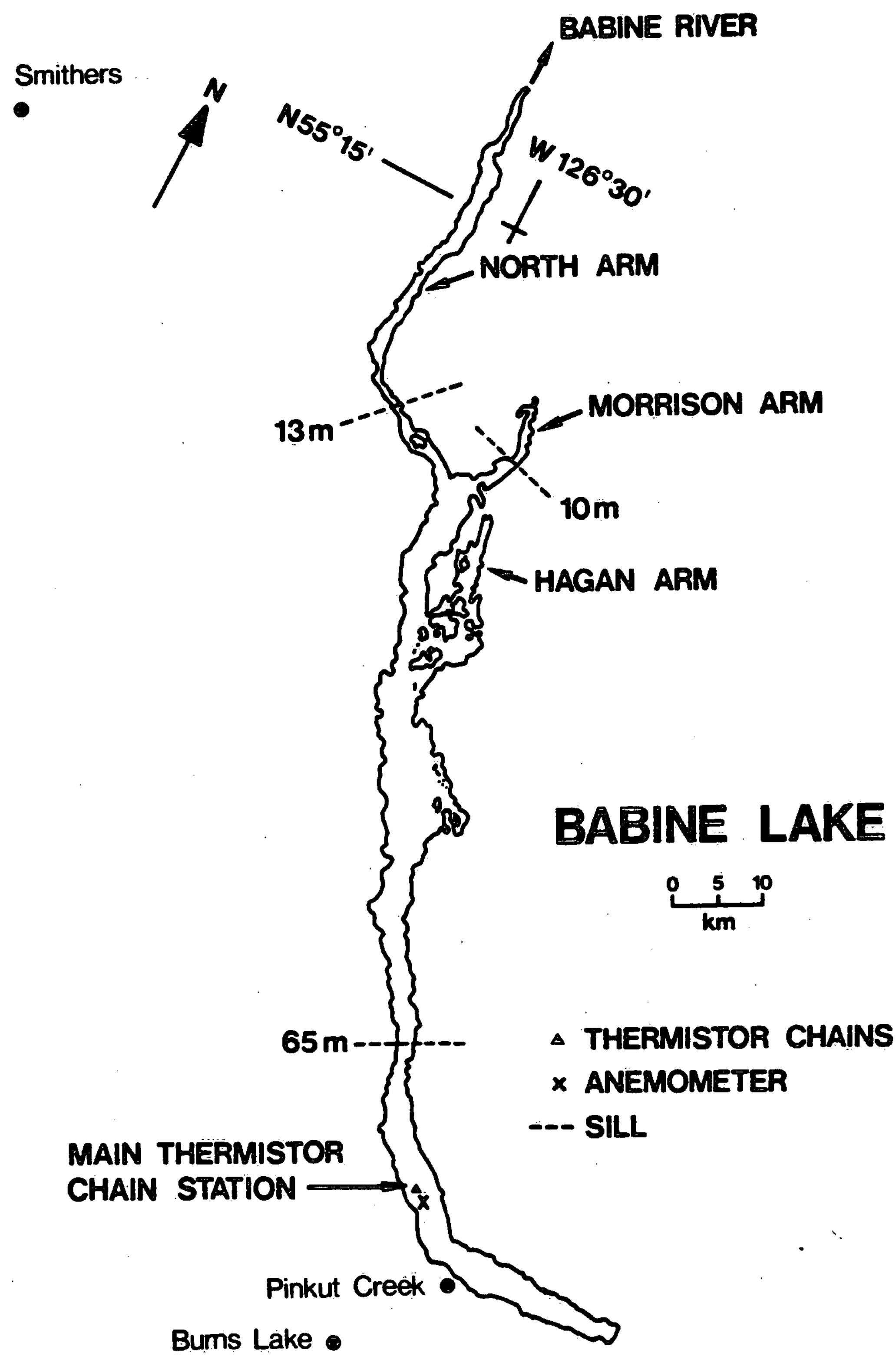
BABINE RIVER
Smithers
N
N55°15'
W 126°30'
NORTH ARM
MORRISON ARM
13 m
10 m
HAGAN ARM
BABINE LAKE
0 5 10
km
65 m
THERMISTOR CHAINS
ANEMOMETER
SILL
MAIN THERMISTOR
CHAIN STATION
Pinkut Creek
Burns Lake

Fig 4

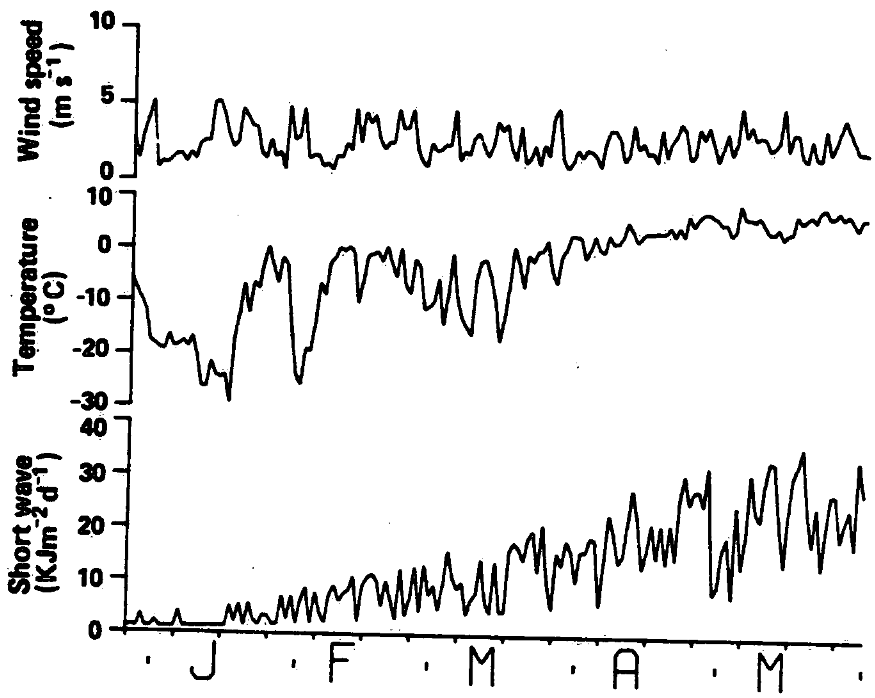

Wind speed
(m s-1)
10
5
0
Temperature
(°C)
10
0
-10
-20
-30
Short wave
(KJm-2 d-1)
40
30
20
10
0
J
F
M
A
M

Fig 3

Fig 5

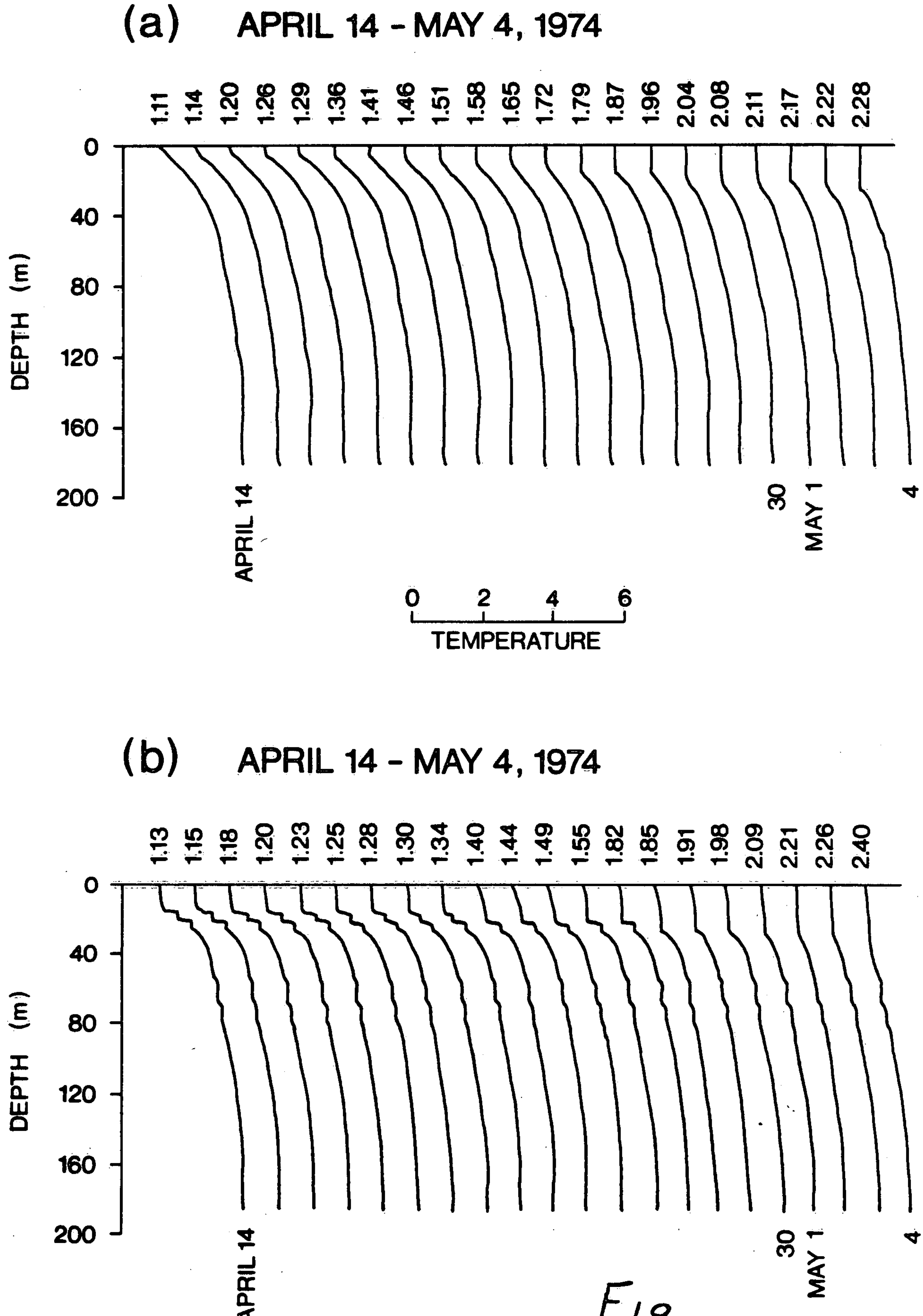
(a) APRIL 14 - MAY 4, 1974
1.11 1.14 1.20 1.26 1.29 1.36 1.41 1.46 1.51 1.58 1.65 1.72 1.79 1.87 1.96 2.04 2.08 2.11 2.17 2.22 2.28
DEPTH (m)
0 40 80 120 160 200
APRIL 14
30
MAY 1
4
0 2 4 6
TEMPERATURE
(b) APRIL 14 - MAY 4, 1974
1.13 1.15 1.18 1.20 1.23 1.25 1.28 1.30 1.34 1.40 1.44 1.49 1.55 1.82 1.85 1.91 1.98 2.09 2.21 2.26 2.40
DEPTH (m)
0 40 80 120 160 200
APRIL 14
30
MAY 1
4

Fig 6

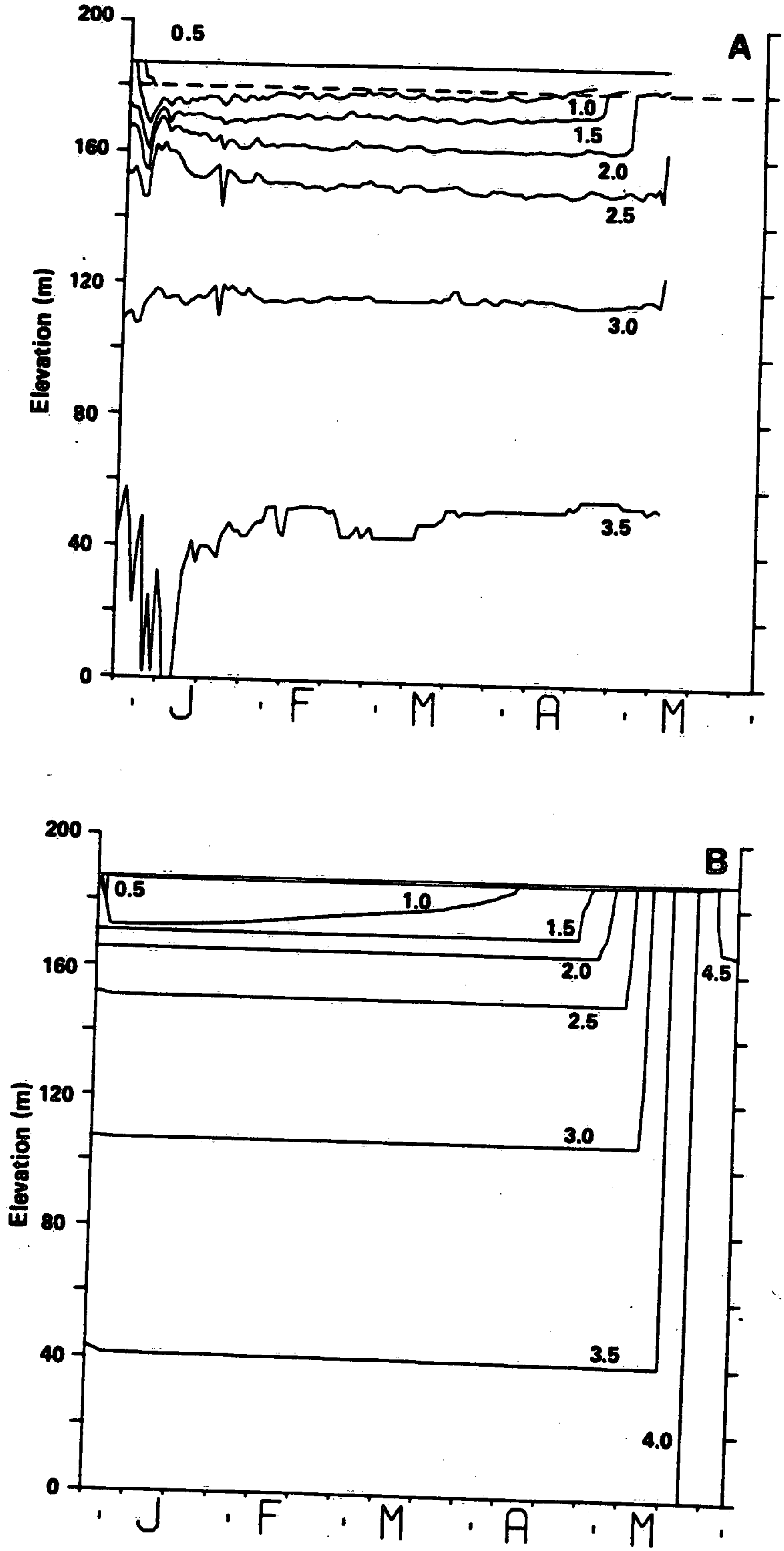

Fig 7

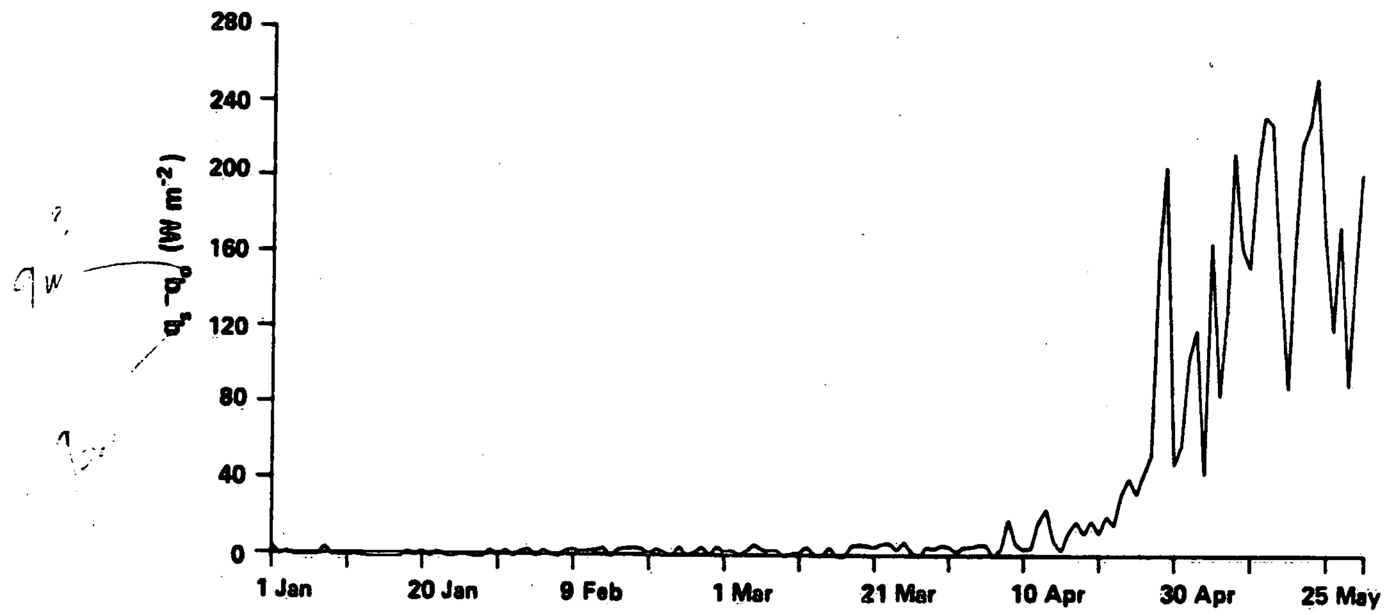
280
240
200
160
120
80
40
0
1 Jan
20 Jan
9 Feb
1 Mar
21 Mar
10 Apr
30 Apr
25 May

Fig 8

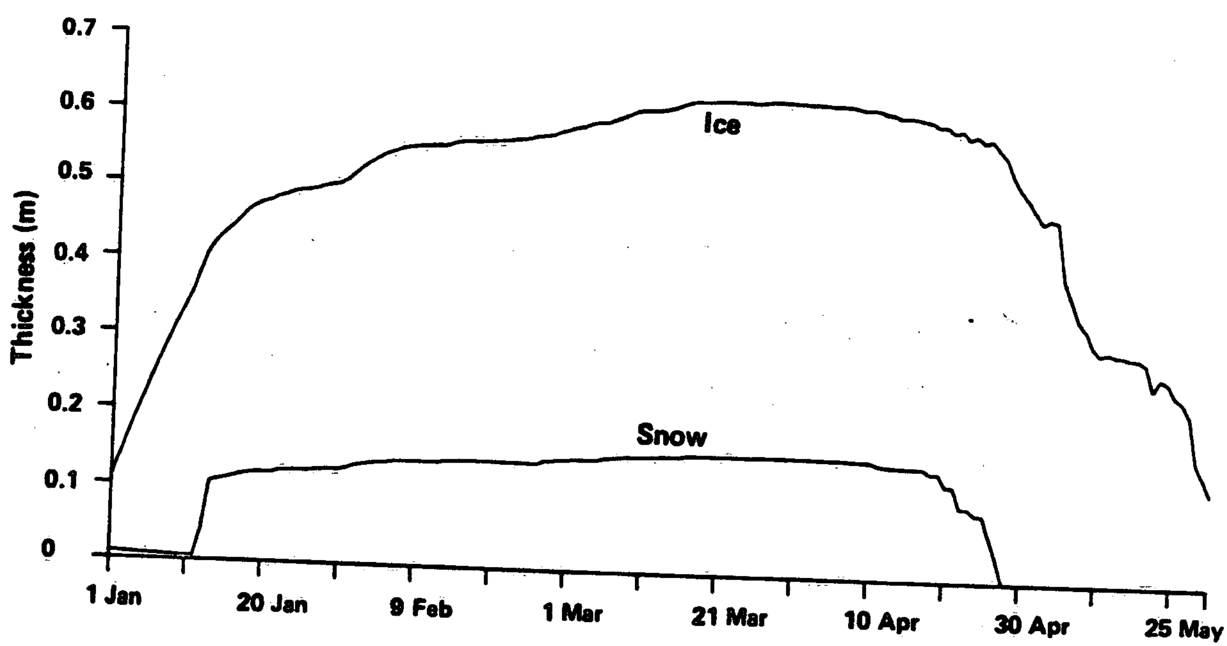
0.7
0.6
0.5
0.4
0.3
0.2
0.1
0
Thickness (m)
Ice
Snow
1 Jan
20 Jan
9 Feb
1 Mar
21 Mar
10 Apr
30 Apr
25 May

Fig 9